Transfer Feasibility Study, Document 1200-59, May 18, 1973, Jet Propulsion Lab., Pasadena, Calif.

[4] Elliott, D. G. and Weinberg, E., *Acceleration of Liquids in Two-Phase Nozzles,* TR 32-987, July 1968, Jet Propulsion Lab., Pasadena, Calif.

[5] Cerini, D. J., "Circulation of Liquids for MHD Power Generation," *Electricity from MHD,* 1968, International Atomic Energy Agency, Vienna, 1968, pp. 2019–2033.

[6] Cerini, D. J. and Elliott, D. G., "Performance Characteristics of a Single Wavelength Liquid Metal MHD Induction Generator with End Loss Compensation," *AIAA Journal,* Vol. 6, No. 3, March 1968, pp. 503–510.

[7] Cerini, D. J. and Elliott, D. G., "Test Results of a NaK-Nitrogen Liquid Metal MHD Converter," *Fifth International Conference on MHD Electrical Power Generation,* Vol. III, International Atomic Energy Agency, Vienna, 1971, pp. 177–192.

[8] Elliott, D. G., Cerini, D. J., Hays, L. G., and Weinberg, E., "Liquid Metal MHD Power Conversion," *Supporting Research and Advanced Development,* Space Programs Summary 37-30, Vol. IV, Jet Propulsion Lab., Pasadena, Calif., Dec. 31, 1964, pp. 116–119.

[9] Elliott, D. G., Hays, L. G., Cerini, D. J., and Bogdanoff, D. W., "Investigation of a Liquid-Metal Magnetohydrodynamic Power System," Fifth Intersociety Energy Conversion Engineering Conference, Sept. 1970, AIAA, New York.

JANUARY 1974 AIAA JOURNAL VOL. 12, NO. 1

Effective Electrical Conductivity and Related Properties of a Nonequilibrium High Pressure MHD Plasma

G. BREDERLOW* AND K. J. WITTE*
Max-Planck-Institut für Plasmaphysik, Garching, Germany

This paper describes measurements of the effective electrical conductivity, the effective Hall parameter, the electron temperature and the electron number density made in an argon-potassium plasma over a wide range of current densities from 1 to 12 amp/cm^2, pressures from 2.1 to 8.2 bar and magnetic inductions from 1.1 to 3.6 Tesla at a gas temperature of 1800 °K and a seed fraction of 0.05%. The aim of these investigations is to find out how well the available theories describing the influence of the magnetic field on the plasma properties mentioned can reproduce the experimental data. The measurements showed that in the entire parameter range investigated the theory based on a quasilinear analysis of plane ionization waves and also a semiempirical model agree with the experiment within the measuring accuracy as far as the effective electrical conductivity, the electron temperature and electron number density are concerned.

I. Introduction

THE coupling between the current density and the electron density in a rare-gas-alkali plasma is the reason why it is not possible under MHD generator conditions (crossed electric and magnetic fields) to obtain a stable plasma configuration above a certain critical Hall parameter. Such a plasma is then subject to the discharge structures known as streamers, within which ionization instabilities develop. As outlined in more detail in Ref. 1 the streamers can be considered as zones of elevated current density compared with the corresponding uniform plasma, which are oriented parallel to the mean current direction and are caused by inhomogeneous boundary conditions (segmented electrodes). They are therefore a phenomenon different from the ionization instabilities which are a pure volume effect. Whereas the ionization instabilities reduce the effective electrical conductivity and lead to saturation of the Hall parameter, the streamers do not impair the plasma properties at least in the pressure range of $p \simeq 1$ bar investigated so far.[2] To ensure sufficient accuracy in calculating the performance of a generator in those parameter ranges in which it will have to be operated later in nuclear power stations, an essential requirement is to know the scaling laws for the effective electrical conductivity. For this reason the effective electrical conductivity was experimentally determined for various gas pressures, current densities and magnetic inductions. These results were compared with theoretical values to check which of the various theories describing the influence of ionization instabilities on σ_{eff} best approximates actual conditions. This comparison was taken further by making, at a constant gas pressure, spectroscopic measurements of the electron temperature and electron density as functions of the current density at various magnetic inductions.

Another question of interest here was whether the influence exerted by ionization instabilities on the effective electrical conductivity can be reduced by the streamers when the gas pressure is increased. This is because the extent of the streamers could be decreased on elevation of the pressure since the characteristic length describing the smallest region in which sharp gradients in the plasma properties can form decreases with rising pressure. In the streamers the current density and hence the degree of ionization as well could then increase. If the latter reaches the region of full ionization, it is to be expected that the influence of the ionization instabilities on the effective electrical conductivity will be reduced.

Received May 30, 1973; revision received August 10, 1973. The authors wish to express their gratitude to R. Borde, C. Geisreiter and J. Hartmann for construction of the apparatus and assistance in conducting the experiments. This work was performed under the terms of the agreement on association between Max-Planck-Institut für Plasmaphysik and Euratom.

Index categories: Atomic, Molecular and Plasma Properties; Plasma Dynamics and MHD; Electric Power Generation Research.

* Research Scientist.

II. Theory

This section gives a brief description of the theoretical model used for calculating the dependence of the electrical conductivity, electron temperature, and electron number density on the current density to be compared with the corresponding measurements. The basic quantity of interest is the effective electrical conductivity and also the effective Hall parameter defined by

$$\sigma_{\text{eff}} = [\langle \mathbf{j} \rangle^2 / \langle \mathbf{j} \rangle \cdot \langle \mathbf{E}^* \rangle], \qquad \beta_{\text{eff}} = [\langle E^* \rangle_\perp / \langle E^* \rangle_\parallel]$$

$\langle \mathbf{j} \rangle$ is the current density vector, $\langle \mathbf{E}^* \rangle$ the electric field vector ($\mathbf{V} \times \mathbf{B}$ part included). $\langle E^* \rangle_\perp$ is the component of $\langle \mathbf{E}^* \rangle$ perpendicular to $\langle \mathbf{j} \rangle$ and $\langle E^* \rangle_\parallel$ the component of $\langle \mathbf{E}^* \rangle$ parallel to $\langle \mathbf{j} \rangle$. The notation $\langle \ldots \rangle$ means an instantaneous average over space.

In order to simplify the analysis, three assumptions frequently used are made. Firstly, over the part of the duct where the measurements are made, the properties of the heavy gas particles (argon atoms, potassium atoms, and ions) are uniform in space and stationary in time so that only the electron gas need be considered. Secondly, the plasma is uniform in the direction of the magnetic field so that only variations in the plane normal to this direction are possible. However, it was found in Ref. 1 that there exist structureless, randomly distributed inhomogeneities along the magnetic field lines if the magnetic field is larger then the value beyond which ionization instabilities occur. But there is some evidence (see Sec. V) that these inhomogeneities do not seriously affect the plasma properties so that for the sake of simplicity one may disregard them in the theory.

Thirdly, the plasma behavior is such that at each point in space and at every moment the free and valence electrons are in equilibrium at the electron temperature. Under these conditions the relations needed are the spatially averaged Saha equation, the spatially averaged energy equation, an equation relating the effective electrical conductivity to the spatially averaged electron temperature, electron number density, and spatially averaged Hall parameter. All the averages are instantaneous averages over space (indicated by brackets $\langle \cdots \rangle$) and should be performed over a volume large compared with the 3rd power of a characteristic length scale of the plasma inhomogeneities. In this case the average values are practically independent of time as long as the total current flowing through the plasma does not change. When we write for the electron number density

$$N_e(\mathbf{r}, t) = \bar{N}_e\{1 + \tilde{N}_e(\mathbf{r}, t)\}$$

where $\mathbf{r}$ is a vector with the components x, y, z and $\bar{N}_e$ a constant average value then—because of the assumption of a large integration volume—it holds

$$\langle N_e(\mathbf{r}, t) \rangle \simeq \bar{N}_e = \text{const}$$

so that

$$N_e(\mathbf{r}, t) = \langle N_e \rangle \{1 + \tilde{N}_e(\mathbf{r}, t)\}, \quad \langle \tilde{N}_e \rangle = 0, \quad \text{but} \quad \langle \tilde{N}_e^2 \rangle \neq 0$$

Similar relations are valid for the electron temperature T_e and the other plasma properties.

In each point of space the Saha equation reads

$$N_e(\mathbf{r}, t) = -\tfrac{1}{2} f_s + (\tfrac{1}{4} f_s^2 + N_K^0 f_s)^{1/2}$$

where

$$f_s = \left(\frac{m_e k T_e(\mathbf{r}, t)}{2\pi h^2}\right)^{3/2} \exp\left\{-\frac{\varepsilon_i}{k T_e(\mathbf{r}, t)}\right\}$$

Here N_K^0 means the total number density of potassium atoms, m_e the electron mass, k Boltzmann's constant, h Planck's constant and ε_i the ionization energy of potassium. Carrying out the averaging procedure

$$\langle N_e \rangle = -\tfrac{1}{2} \langle f_s(T_e) \rangle + \langle (\tfrac{1}{4} f_s^2 + N_K^0 f_s)^{1/2} \rangle$$

by using the relations for N_e introduced above we arrive at

$$\langle N_e \rangle = N_e(\langle T_e \rangle)\{1 + a \langle \tilde{T}_e^2 \rangle\}$$

where higher order terms in $\tilde{T}_e$ have been neglected. The factor a is about 30 at $\langle T_e \rangle = 3000°\text{K}$ and becomes lower with rising T_e. According to the known fluctuation measurements $\langle \tilde{T}_e^2 \rangle$ can be approximated by the value $\lesssim 0.001$ so that in the current density range of interest we obtain with an accuracy of at least 3%

$$\langle N_e \rangle = N_e(\langle T_e \rangle) = -f_s(\langle T_e \rangle)/2 + [\tfrac{1}{4} f_s(\langle T_e \rangle)^2 + f_s(\langle T_e \rangle) N_K^0]^{1/2} \tag{1}$$

In the case of the energy equation

$$[\langle \mathbf{j} \rangle^2 / \sigma_{\text{eff}}] = \langle \dot{E}_{el} \rangle + \langle \dot{E}_R \rangle \tag{2}$$

similar considerations lead to the result that the elastic losses and the radiation losses can also be calculated by using only the average values $\langle N_e \rangle$, $\langle T_e \rangle$, etc., and neglecting the contributions arising from higher order terms like $\langle \tilde{T}_e^2 \rangle$, $\langle \tilde{N}_e^2 \rangle$ or $\langle \tilde{T}_e \tilde{N}_e \rangle$

$$\langle \dot{E}_{el} \rangle = 3k \langle N_e \rangle (\langle T_e \rangle - T_g) \langle \nu \rangle m_e / m_A$$

$$\langle \dot{E}_R \rangle = 2\pi(h+d)/hd \{B_\lambda(\langle T_e \rangle) - B_\lambda(T_w)\} \Delta\lambda$$

with

$$T_w = T_g - 300°$$

Here T_g means the gas temperature, $\langle \nu \rangle$ the average collision frequency, m_A the mass of an argon atom, h the duct height, d the extent of the duct in the direction of the magnetic field, B_λ Planck's function, and T_w the wall temperature.

For the same reasons as previously mentioned the average collision frequency $\langle \nu \rangle$ can be approximated by

$$\langle \nu \rangle = (8k \langle T_e \rangle / \pi m_e)^{1/2} \{\tfrac{4}{3} N_A Q_{e-A}(\langle T_e \rangle) +$$

$$\tfrac{4}{3}(N_K^0 - N_e) Q_{e-K}(\langle T_e \rangle) + \langle N_e \rangle Q_{e-I}(\langle N_e \rangle, \langle T_e \rangle)\}$$

where N_A is the number density of the argon atoms and the Q_{e-i} the velocity averaged cross section. Q_{e-A} was determined with the data from Ref. 9. In the electron temperature range of interest $2000 \leqq \langle T_e \rangle \leqq 4000°\text{K}$ it can be obtained from the relation

$$Q_{e-A}(\langle T_e \rangle) = -0.29 + 0.42 \cdot 10^{-3} \langle T_e \rangle \ [\text{Å}^2], \ \langle T_e \rangle \text{ in } [°\text{K}]$$

The electron-ion collision cross section Q_{e-I} was calculated according to the formula[10]

$$Q_{e-I}(\langle N_e \rangle, \langle T_e \rangle) = \frac{2.96 \cdot 10^{10}}{\langle T_e \rangle^2} \ln\left\{1.24 \cdot 10^7 \left(\frac{\langle T_e \rangle^3}{\langle N_e \rangle}\right)^{1/2}\right\} \text{ in } [\text{Å}^2]$$

with $\langle T_e \rangle$ in $[°\text{K}]$ and N_e in $[\text{m}^{-3}]$. In the electron temperature range of interest, $2200 \leqq \langle T_e \rangle \leqq 3600$, the electron potassium cross section Q_{e-K} can be approximated by

$$Q_{e-K}(\langle T_e \rangle) = 360 - 58 \cdot 10^{-3} \langle T_e \rangle \text{ in } [\text{Å}^2], \ \langle T_e \rangle \text{ in } [°\text{K}]$$

This formula was derived from the results for $Q_{e-K}(\langle T_e \rangle)$ obtained by Raeder,[11] whose calculations are based on the theoretical investigations[12,13] and which agreed satisfactorily with the experimental data.[14,15]

The formula for the radiation loss $\dot{E}_R$ was taken from Ref. 8. The quantity $\Delta\lambda$ can be considered as measure of the line width and is given by

$$\Delta\lambda = (25 + 10^4 c)(p_g / p_g^R)^{1/2}$$

where c is the seed fraction, p_g the gas pressure, and p_g^R a reference pressure, in our case 1 bar.

Finally, we present the various equations relating the effective electrical conductivity to the spatially averaged values of the electrical conductivity $\langle \sigma \rangle$ and the Hall parameter $\langle \beta \rangle$

$$\sigma_{\text{eff}} = \begin{cases} \langle \sigma \rangle \dfrac{\sigma_N + (\sigma_N^2 + \beta_{\text{crit}}^2)^{1/2}}{\sigma_N + (\sigma_N^2 + \langle \beta \rangle^2)^{1/2}} & \text{(Ref. 3)} \quad (3a) \\ \langle \sigma \rangle \dfrac{(\sigma_N^2 + \beta_{\text{crit}}^2)^{1/2}}{(\sigma_N^2 + \langle \beta \rangle^2)^{1/2}} & \text{(Ref. 4)} \quad (3b) \\ \langle \sigma \rangle \dfrac{\beta_{\text{eff}}}{\langle \beta \rangle} & \text{(Ref. 5)} \quad (3c) \\ \langle \sigma \rangle \dfrac{\beta_{\text{crit}}}{\langle \beta \rangle} & (3d) \\ \sigma_0 \left[\dfrac{\beta_{\text{crit}}}{\beta_0 (2)^{1/2}}\right]^{1/2} & \text{valid for } \beta_0 \gtrsim 5\beta_{\text{crit}} \quad \begin{cases}\text{(Ref. 6)} \\ \text{(Ref. 7)}\end{cases} \quad (3e) \end{cases}$$

Again $\langle\sigma\rangle$ and $\langle\beta\rangle$ can be approximated by

$$\langle\sigma\rangle = (e^2\langle N_e\rangle/m_e\langle\nu\rangle)f(\langle T_e\rangle, \langle\beta\rangle), \qquad \langle\beta\rangle = (eB/m_e\langle\nu\rangle)$$

where e is the electron charge and $\mathbf{B}$ the magnetic induction. The calculation of $\langle\sigma\rangle$ had to allow for the fact that in a plasma with collision cross sections dependent on the electron energy the value of $\langle\sigma\rangle$ decreases if a transverse magnetic field is applied. This influence is accounted for by the factor $f(\langle\beta\rangle, \langle T_e\rangle)$. This reduction factor was calculated for the present conditions using the Frost-Schweitzer-Mitchner rule as described in Ref. 16.

In Eqs. (3a–e) β_{crit} is the critical Hall parameter beyond which the plasma becomes unstable and σ_N is a logarithmic derivative

$$\beta_{crit} = \left(\left.\frac{d\ln \dot{E}_{el}}{d\ln N_e}\right|_{\substack{T_e=\langle T_e\rangle \\ N_e=\langle N_e\rangle}} - \sigma_N{}^2\right)^{1/2} \qquad \sigma_N = \left.\frac{d\ln\sigma}{d\ln N_e}\right|_{\substack{T_e=\langle T_e\rangle \\ N_e=\langle N_e\rangle}}$$

When the plasma is stable ($\beta < \beta_{crit}$) σ_{eff} becomes equal to $\langle\sigma\rangle$ and the effective Hall parameter equal to the spatially averaged $\langle\beta\rangle$. Because there is no difference between the microscopic and macroscopic quantities in this case the notation $\langle\cdots\rangle$ can also be omitted.

The first two expressions for the effective electrical conductivity Eqs. (3a) and (3b) were obtained from a quasilinear analysis of plane ionization waves with the assumption of small fluctuations in N_e. The different results arise from a different linearization procedure which in Ref. 3 finally leads to an underestimation of the dissipation losses caused by the ionization instabilities as will be shown later. It comes from a different choice of the position of the coordinate system relative to the plasma striations. Whereas in Ref. 4 the striations are always perpendicular to the x-axis, in Ref. 3 the averaged current density $\langle\mathbf{j}\rangle$ coincides with the x-axis. The latter choice has the consequence that the perturbation current is no longer a linear function of the other perturbation quantities; mixed terms appear which can only be removed by making the additional assumption of square waves which is not a necessary assumption in Ref. 4 in order to arrive at the formula Eq. (3a) for the effective electrical conductivity.

For a highly unstable plasma ($\langle\beta\rangle \gg \beta_{crit}$) consisting of "two phases" whereby the volumes occupied by the phases are equal and their locations are random an exact calculation of the effective electrical conductivity was carried out in Ref. 5 yielding Eq. (3c). Because the mean square value $\langle\tilde{\sigma}^2\rangle$ of the fluctuations in σ enters the calculation of β_{eff}, but cannot be determined from Dykhne's theory and has therefore to be taken from experiments, Eq. (3c) can only be checked by simultaneous measurement of σ_{eff} and β_{eff}. Because it was not possible in our experiment to measure β_{eff} with an accuracy such as would have allowed a check on the applicability of Eq. (3c) we made no attempt to investigate Dykhne's model any further.

Equation (3d) can be formally derived from Eqs. (3a) and (3b) by assuming a Coulomb collision dominated plasma ($\sigma_N \simeq 0$), but Eq. (3d) can also be considered as a semiempirical description of the dependence of σ_{eff} on the spatially averaged plasma properties, valid also for a slightly ionized plasma. Equation (3e) was derived by assuming a model of the discharge pattern which consists of two orthogonal families of equidistant parallel striations oriented at $\pm\pi/4$ to the vector of the mean current. The quantities σ_0 and β_0 refer to a stable, i.e., ionizational fluctuation-free plasma having a uniform current density just equal to the average current density in the unstable plasma under investigation. σ_0 and β_0 are not equal to $\langle\sigma\rangle$ and $\langle\beta\rangle$. Because at the same current density the electron temperature in the stable plasma is smaller than in the unstable plasma $\sigma_0 < \langle\sigma\rangle$ and $\beta_0 < \langle\beta\rangle$ holds. We have calculated σ_{eff} according to Eq. (3e) in its range of applicability $\beta_0 \gtrsim 5\beta_{crit} \approx 7$ and found good agreement with the values obtained from Eqs. (3a) and (3c). This result allows a restriction of the following considerations on the Eqs. (3a–c).

When σ_{eff} is plotted vs $\langle j\rangle$, a different curve is obtained for every value of the gas pressure p_g and magnetic induction B. All these curves, however, can be combined in one by assuming a slightly ionized plasma whose effective electrical conductivity is described by Eq. (3d), and in which the radiation losses can be neglected relative to the elastic losses. Under our experimental conditions this situation is largely present. First it follows from Eq. (3d) that at constant seed fraction and gas temperature

$$\sigma_{eff} = [(p_g)^{1/2}/B]g_\sigma(\langle T_e\rangle)$$

where β_{crit} is assumed to be independent of the gas pressure p_g. Inserting this relation in the energy Eq. (2) yields

$$\langle j\rangle = [p_g/(B)^{1/2}]g_j(\langle T_e\rangle)$$

g_σ and g_j are two functions that depend only on the electron temperature and on nothing else. This means, however, that only a single curve is obtained for every value of the pressure p_g and magnetic induction B when the reduced electrical conductivity $\sigma_{eff}B/(p_g)^{1/2}$ is plotted vs the reduced current density $\langle j\rangle(B)^{1/2}p_g$.

III. Experimental Conditions and Apparatus

The measurements were made in the generator duct of a simulated Faraday-Type MHD generator operated with an Ar-K mixture. The gas temperature was $T_g = 1800°K$, the pressure in the range $2.1 \leqq p_g \leqq 8.2$ bar, the mass flow rate 73–82 g/sec, the average flow velocity $50 \leqq V \leqq 240$ m/sec, and the seed concentration $C = 0.05\%K$. A transverse magnetic field with an induction of up to $3.6T$ was applied.

The current was sent through the plasma transversely to the flow direction. It was caused by external electric fields applied separately to the individual electrode pairs in the direction of the $v \times B$ emf. The duct was made of Al_2O_3, the cross section being 20×30 mm^2 and the length 100 mm. Thirty-two circular electrodes 1 mm in diameter with periodicity intervals of $s = 3$ and $s = 6$ mm were used. To keep the relaxation length short, four specially arranged electrodes were placed in the entrance region of the duct (Fig. 1). Periodic conditions could then be achieved 30 mm downstream from the inlet region.

IV. Measuring Methods and Data Reduction

a) Effective Electrical Conductivity and Effective Hall Parameter

The effective electrical conductivity σ_{eff} and the effective Hall parameter β_{eff} were calculated from the electric field vector $\langle\mathbf{E}^*\rangle = \langle\mathbf{E}\rangle + \langle\mathbf{v}\rangle \times \mathbf{B}$ and the current density vector $\langle\mathbf{j}\rangle$ according to Ohm's law

$$\sigma_{eff} = \sigma_{app}(1 + tg\gamma\beta_{eff})$$
$$\beta_{eff} = (\beta_{app} + tg\gamma)/(1 - \beta_{app}\, tg\gamma)$$
$$\langle j\rangle \simeq \langle j_y\rangle(1 + 0.5tg^2\gamma)$$

where the definitions

$$\sigma_{app} = \langle j_y\rangle/(\langle E_y\rangle + vB)$$
$$\beta_{app} = \langle E_x\rangle/(\langle E_y\rangle + vB)$$
$$tg\gamma = \langle j_x\rangle/\langle j_y\rangle$$

have been used. γ is the average angle which the current density vector forms with the y direction in the region of the probes.

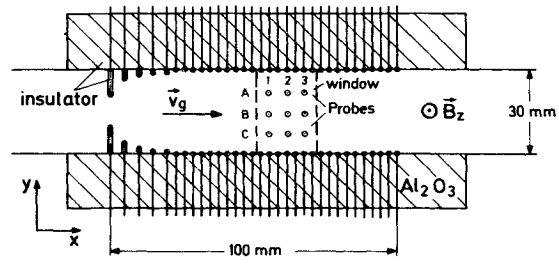

Fig. 1 Diagram of the measuring duct.

γ was determined from the direction of the streamers,[1] which coincides with the current direction. The orientation of the streamers was obtained from image converter pictures made simultaneously with the probe measurements in the direction of the magnetic field lines through a window in the side wall (Fig. 1). γ was usually in the range $3° \lesssim \gamma \lesssim 12°$, the value increasing with decreasing current density and, to a less extent, with increasing magnetic induction. This way of determining γ is not very precise, the accuracy being of the order of $\pm 25\%$. This has a strong effect on the magnitude of β_{eff}, a far less pronounced one on the magnitude of σ_{eff} and an almost negligible one on the magnitude of $\langle j \rangle$.

At pressures above 3.8 bar no image converter pictures were taken. In this case it was assumed that the current direction for equal $\langle \beta \rangle$ and $\langle j \rangle$ is the same as under those circumstances where the direction of $\langle j \rangle$ could be read from image converter pictures. This assumption looks reasonable in view of the fact that the relaxation effects should not change dramatically because of two counterbalancing effects, the one being the decreasing gas velocity (the mass flow rate stays constant) and the other the decreasing electrical conductivity.

$\langle E_y \rangle$ and $\langle E_x \rangle$ were determined from the probe signals as an average value over 6 Faraday voltages (Fig. 1, A1-B1, A2-B2, A3-B3, B1-C1, B2-C2, and B3-C3) and four Hall voltages (A1-A2, A2-A3, C1-C2, and C2-C3) divided by the corresponding distance of the probes between which the voltage was measured. They were simultaneously recorded together with the current I_y and the magnetic induction B. In the case of $\langle E_y \rangle$ the mean square root deviation from the average values was 1% at $B = 0$, and 4% at $B > 0$, and in case of $\langle E_x \rangle$ 2%. The $v \times B$ emf was derived from the probe signals under open circuit conditions. This value was checked with the result which was obtained from a separate measurement of the magnetic induction B and the gas velocity v calculated from the simultaneously recorded values of the mean flow rate, the static gas pressure and temperature. Within the experimental accuracy both methods yielded the same result.

The current density $\langle j_y \rangle$ was determined from the total current I_y (averaged over the five electrode pairs in the region of the probes) and the cross-sectional area $F = sd$, s being the electrode pitch. Because there is no current flowing in the boundary layers along the side walls, the effective area F_{eff} is smaller than F. According to Ref. 8 we have assumed $F_{\text{eff}} = (0.95 \pm 0.02)F$. The error margins of the current density $\langle j \rangle \simeq I_y/F_{\text{eff}}$ are essentially due to this uncertainty regarding the thickness of the boundary layer because the variations of I_y over the electrode pairs considered were less than 1%.

To sum up, the following error margins can be given: a) effective electrical conductivity σ_{eff}: $\pm 5\%$ at $B = 0$, $\pm 8\%$ at $B > 0$, b) effective Hall parameter β_{eff}: $\pm 15\%$, and c) current density $\langle j \rangle$: $\pm 3\%$.

b) Electron temperature

The electron temperature was derived from the measurement of the potassium resonance radiation ($\lambda_0 = 766.5$ nm). For this purpose the opening in the side wall for allowing image converter pictures to be taken was covered with an Al_2O_3 plate which for this measurement was provided in the center with an aperture having a diameter of 2.5 mm. The radiation escaping from the plasma through this aperture was focused on the entrance slit of a monochromator with a bandpass between 2 and 10 Å, which isolated the potassium resonance radiation from the remainder of the spectrum. The radiation leaving the monochromator was fed into a photomultiplier tube whose output was displayed as a function of time by means of an x-y recorder. This quantity can be considered as a relative measure of the potassium resonance radiation and—as will be shown later—also of the electron temperature averaged over time and the area of the aperture. When the average over time

$$[T_e] = \frac{1}{t_s}\int_0^{t_s} T_e(\mathbf{r}, t)\, dt$$

is carried out over a time scale t_s much larger than the one pertaining to the ionization instability as it was in our case then because of $T_e(\mathbf{r}, t) = \bar{T}_e\{1 + \tilde{T}_e(\mathbf{r}, t)\}$ and $\langle T_e \rangle = \bar{T}_e$ it holds $\langle T_e \rangle = [T_e]$. When the radiation of the central regions of the potassium resonance lines, to which the plasma is optically very thick, is used for the measurement of the electron temperature, pure argon had to be blown in through the viewing aperture to remove the absorbing potassium from the colder boundary. The flow rate of argon $\dot{m}_A$ to be blown in was found by investigating the intensity I_λ as a function of the wavelength λ. When $\dot{m}_A$ was about equal to or larger than 1 gr/s the effect of self-absorption disappeared and the maximum of the intensity was in the line center, as is expected in the absence of electron temperature gradients (isothermal plasma).

The measurements were also made in the line wings, to whose radiation the plasma is transparent. In this case no purge flow is necessary, at least in principle. Within the experimental accuracy equal results were obtained for the electron temperature. This agreement confirms our conclusion that with a sufficiently strong purge flow the plasma can be considered as almost isothermal with regard to the electron temperature.

Assuming an isothermal plasma, the resonance radiation intensity I_λ emitted by the plasma through the aperture can be derived from integration of the radiation transport equation, thus yielding

$$I_\lambda^A = I_\lambda^W(T_w)\exp(-\alpha_\lambda d/\cos\phi) + I_\lambda^P \simeq I_\lambda^P = B_\lambda(T_p)\{1 - \exp(-\alpha_\lambda d/\cos\phi)\}\dagger \qquad (4)$$

The total radiation consists of the two contributions, wall radiation $I_\lambda^W \exp(-\alpha_\lambda d/\cos\phi)$ (wall opposite the aperture) and plasma radiation I_λ^P. Because the wall temperature T_w is much smaller than the population temperature T_p we neglect the wall radiation compared with the plasma radiation. d is the duct width and ϕ the angle between the normal of the aperture (direction of $\mathbf{B}$) and the ray considered. Since the absorption coefficient α_λ is practically independent of T_p, the plasma emits like a black body as regards the temperature. It was shown in Ref. 17 that under our experimental conditions the population temperature T_p is practically equal to the electron temperature. The energy flow $\dot{E}$ (energy per unit time) received by the photomultiplier tube and displayed on the x-y recorder can be obtained from Eq. (4)

$$E = \pi F_A \bar{\phi}^2 B_{\lambda M}(T_e)\int_{\lambda_1}^{\lambda_2}(1 - e^{-\alpha_\lambda d})\, d\lambda = \text{const}\, B_{\lambda M}(T_e) \qquad (5)$$

where use has been made of the fact that here ϕ is a small angle and Planck's function has been set constant in the integration interval and equal to the value determined at $\lambda_M = \frac{1}{2}(\lambda_1 + \lambda_2)$. F_A is the area of the aperture and $\bar{\phi}$ the half-apex-angle of the cone into which the radiation considered is emitted. $\bar{\phi}$ is given by the characteristics of the optical system used. λ_1 and λ_2 are determined by the adjustment of the monochromator. Equation (5) allows a direct evaluation of the electron temperature $\langle T_e \rangle$ if $\langle T_e \rangle$ is known for one value of the energy flow $\dot{E}$. The necessary calibration was done at high current densities without a magnetic field by assigning the calculated electron temperature to the energy flow $\dot{E}$ measured at the respective current density. The data thus obtained were checked by measuring the energy flow at $\langle j \rangle = 0$ and comparing the corresponding population temperature with the temperature measured with a thermocouple ($\langle T_e \rangle \simeq T_g$). The error margins are larger at lower electron temperatures than at higher ones, but should not exceed ± 35°K.

c) Electron Number Density

The measurement of the recombination continuum was used to determine the relative change of the electron number density $\langle N_e \rangle|_{B>0}/\langle N_e \rangle|_{B=0}$ at constant current density. Here the nota-

† In deriving Eq. (4), α_λ has been assumed constant along the integration path, thereby neglecting the influence of the gas temperature T_g on α_λ by means of the line shape, which is permissible in our case because the variation of T_g across the duct is less than 20%.

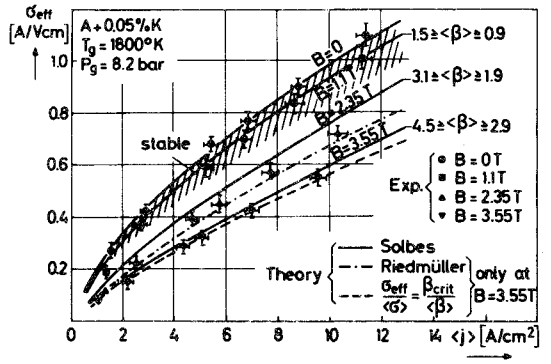

Fig. 2 Effective electrical conductivity as a function of the current density at various magnetic inductions ($p = 8.2$ bar).

tion denotes an average over the area of the aperture and time. The experimental setup was the same as the one used for the measurement of the electron temperature. The monochromator was adjusted at a center wavelength $\lambda = 440$ nm with a band pass of $\Delta\lambda = 2$ nm at half-intensity. In this wavelength range the radiation emitted by the plasma is essentially due to the transition free $-{}^2P_{1/2}$ or free $-{}^2P_{3/2}$, the contributions from free to excited states of higher order no longer being of importance at this wavelength.

The photon energy emission coefficient J_λ (energy per unit time, per unit volume, per unit wavelength, per unit solid angle) can be expressed as

$$J_\lambda = a\frac{(2\pi h)^2 c_L}{m_e}\left(\frac{m_e}{2\pi k T_e}\right)^{3/2}\exp\left\{\frac{2\pi h c_L}{k T_e}\left(\frac{1}{\lambda_1}-\frac{1}{\lambda}\right)\right\}\frac{N_e^2}{\lambda} \tag{6}$$

In deriving this equation a Maxwellian electron distribution function has been assumed[18] and also that the cross section Q for the transition considered is given by the relation $Q = a/v^2$ where v is the electron speed. $\lambda_1 = 454$ nm is the wavelength below which the continuum radiation considered starts. Because the plasma is optically thin to this radiation the radiation transport equation can be integrated without taking the absorption into account. The intensity $I_\lambda{}^A$ released by the plasma through the aperture is then

$$I_\lambda{}^A = I_\lambda{}^W(T_w) + I_\lambda{}^P = \varepsilon_\lambda B_\lambda(T_w) + J_\lambda d/\cos\phi \tag{7}$$

Here the boundary condition $I_\lambda{}^W(T_w) = \varepsilon_\lambda B_\lambda(T_w)$ has been used, where ε_λ is the emissivity coefficient of the Al_2O_3 wall. d and ϕ have the same meaning as in Sec. IV.b. Similarly, the energy flow $\dot{E}$ received by the photomultiplier tube is given by

$$\dot{E} = \dot{E}_w + \dot{E}_p = \pi F_A \bar{\phi}^2 \Delta\lambda (I_\lambda{}^W + I_\lambda{}^P) \tag{8}$$

A numerical calculation of $\dot{E}$ with the constant a taken from Ref. 18 and the assumption $a_{\text{cesium}} \simeq a_{\text{potassium}}$ reveals that at low current densities $\langle j\rangle \simeq 1$ A/cm^2 the wall radiation $\dot{E}_w$ and the plasma radiation $\dot{E}_p$ are of the same order of magnitude. Because we are only interested in $\dot{E}_p$, but not in $\dot{E}_w$, its contribution given by the photomultiplier output at $\langle j\rangle = 0$ (the plasma radiation is then negligible) has to be subtracted from the total radiation $\dot{E}$.

From Eqs. (6) and (7) the ratio $\langle N_e\rangle_{B>0}/\langle N_e\rangle_{B=0}$ can be expressed as

$$\frac{\langle N_e\rangle_{B>0}}{\langle N_e\rangle_{B=0}} = \left(\frac{\langle T_\lambda{}^P\rangle_{B>0}}{\langle I_\lambda{}^P\rangle_{B=0}}\right)^{1/2}\left(\frac{\langle T_e\rangle_{B>0}}{\langle T_e\rangle_{B=0}}\right)^{3/4}\times \exp\left(T_R\left[\frac{1}{\langle T_e\rangle_{B>0}}-\frac{1}{\langle T_e\rangle_{B=0}}\right]\right) \tag{8a}$$

where

$$T_R = \frac{2\pi h c_L}{k}\left(\frac{1}{\lambda}-\frac{1}{\lambda_1}\right) \simeq 500°\text{K} \tag{8b}$$

In Eq. (8a) contributions due to fluctuations in T_e have been neglected because they are small. At constant current density the electron temperature is higher in an unstable plasma than in a stable one owing to the influence of ionization instabilities caused by applying an external magnetic field. As will be shown later, $\langle T_e\rangle_{B>0}$ (see Fig. 6) will not exceed $\langle T_e\rangle_{B=0}$ by more than 10% for all the cases investigated (at constant current density). In Eq. (8a) we may therefore approximate the value of the terms containing the electron temperature by 1 so that together with Eq. (8)

$$\langle j\rangle = \text{const}: \frac{\langle N_e\rangle_{B>0}}{\langle N_e\rangle_{B=0}} \simeq \left(\frac{\langle I_\lambda{}^P\rangle_{B>0}}{\langle I_\lambda{}^P\rangle_{B=0}}\right)^{1/2} = \left(\frac{(\dot{E}-\dot{E}_w)_{B>0}}{(\dot{E}-\dot{E}_w)_{B=0}}\right)^{1/2}$$

The resulting error of the relative change of the electron number density due to this approximation is less than 10%.

V. Discussion of the Results

a) Effective Electrical Conductivity

The effective electrical conductivity was measured at pressures of 2.1, 3.9, 6.9, and 8.2 bar and magnetic inductions of $B = 0$, 1.1, 2.35 and 3.55 tesla in the current density range 1 to 12 amp/cm^2. At $B = 0$ there was always good agreement between theory and experiment. The measurements showed that in the entire pressure range there are no essential differences in the shapes of the curves. Therefore, as a typical example only the conductivity curve recorded at $p = 8.2$ bar is reproduced here (Fig. 2). The various test points with their margins of error are drawn for the various magnetic inductions. The solid curves represent the conductivity values calculated with Eq. (3b) according to Solbes' theory[4] for the various magnetic inductions ($B = 1.1$, 2.35 and 3.55 T). For $B = 3.55$ T, the curves calculated with the expression given by Riedmüller[3] for σ_{eff} [Eq. (3a)] and with the relation $\sigma_{\text{eff}}/\langle\sigma\rangle = \beta_{\text{crit}}/\langle\beta\rangle$ Eq. (3d) are also given. In all cases $\langle\sigma\rangle$, β_{crit}, and $\langle\beta\rangle$ have been calculated according to the formulas given in Sec. II. For the sake of clearness in Fig. 2 the curve corresponding to Eq. (3e) has been omitted because it lies between the curves representing Eqs. (3b) and (3d). Whereas the values obtained with Eqs. (3b, 3d, and 3e) closely approximated the measured values both here and in the other pressure ranges investigated, the curves calculated with Eq. (3a) always exceeded the experimental values. This is in agreement with the results in Ref. 2, where the current-voltage characteristics of the generator calculated with Solbes' formula Eq. (3b) and Eq. (3d) reproduced the experimental data reasonably well, whereas Riedmüller's

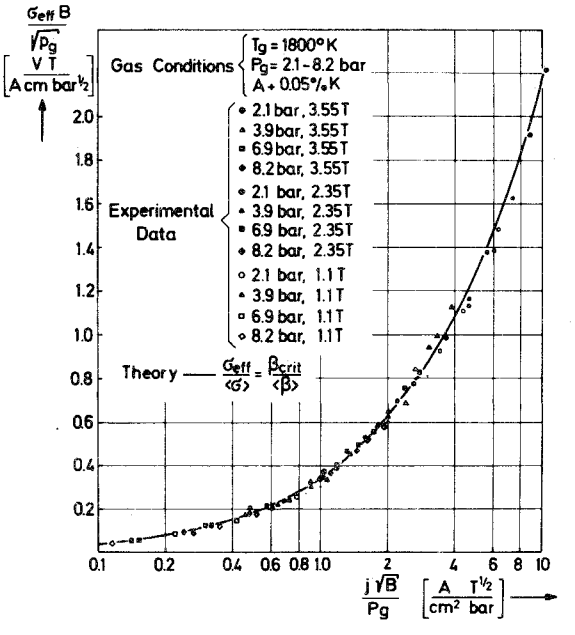

Fig. 3 Reduced effective electrical conductivity $\sigma_{\text{eff}} B/(p_g)^{1/2}$ as a function of the reduced current density $\langle j\rangle(B)^{1/2}/p_g$, at various pressures and magnetic inductions.

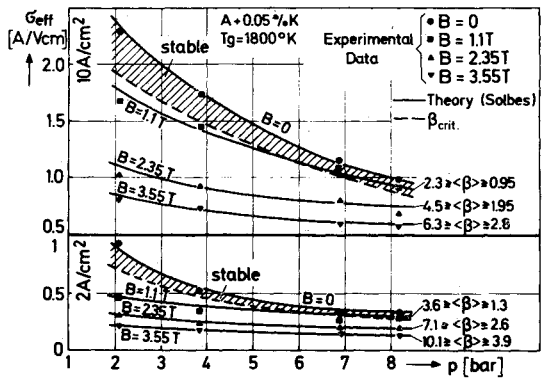

Fig. 4 Effective electrical conductivity as a function of the pressure at various magnetic inductions and current densities.

formula Eq. (3a) always overestimated the generator performance.

At low magnetic induction ($B = 1.1$ T) and relatively high pressure the Hall parameter was lower than the critical value. Ionization instabilities therefore did not yet occur. The effective conductivity is nevertheless below that without magnetic field, this being due to the fact that in an argon-potassium plasma the scalar electrical conductivity is reduced when a transverse magnetic field is applied. In Fig. 3 the reduced effective electrical conductivity is plotted as a function of the reduced current density. The solid curve represents the values calculated with Eq. (3d). Here only the experimental values at which the Hall parameter was higher than the critical value are given. It can be seen that in the entire current density, pressure and magnetic field ranges investigated the experimental values practically coincide with those calculated. This proves that the influence of ionization instabilities on the effective electrical conductivity can be theoretically determined in very good approximation even when the individual parameters are varied over wide ranges.

To demonstrate the dependence of the effective electrical conductivity on the pressure, it was plotted as a function of the pressure for various current densities and magnetic fields (Fig. 4). The solid curves represent the values calculated with the relation (3b). It can be seen that in the unstable region σ_{eff} decreases only slightly with increasing pressure. This is because the Hall parameter becomes smaller with rising pressure. In the entire pressure range the experimentally and theoretically determined values of the conductivity were practically in agreement. But this result should also be viewed in terms of the fact that the gas pressure p_g, the gas temperature T_g and the magnetic induction B, which all enter the theory, have to be the same as in the measurements. But these quantities are known only within certain limits. For p_g the accuracy is $\pm 5\%$, for T_g $\pm 50°$K or $\pm 3\%$ and for $B \pm 0.1$ T. In principle, the seed fraction should also be taken into account, but the plasma properties are not very sensitive to small changes in this quantity.

Finally, reference is made to the consideration expressed in the introduction that because of the decreasing extent of the streamers with increasing pressure there might be a possibility of getting such high current densities in the streamers that the seed becomes fully ionized, that is the fine structure of the streamers caused by the ionization instabilities disappears. This should then have an advantageous effect on the electrical conductivity. However, the experimental results did not confirm this conclusion. This means that the streamers had not become thin enough or the current densities not high enough, or that when the streamers become too thin to allow a fine structure to be built up they disappear and the discharge pattern is only governed by the ionization instabilities. Although the image converter pictures taken at various gas pressures up to 3.9 bar prove that at equal Hall parameter and current density the streamers become thinner with increasing gas pressure this information is not sufficient to answer the question raised.

In this context is is also interesting to point out that the good agreement between the quasi-linear theory of Solbes and the experiment over the entire pressure and Hall parameter ranges investigated, where at the lower pressures the discharge pattern used in the theory because of the omission of the streamers is certainly different from the one actually occurring, seems to indicate that the value of the effective electrical conductivity is not very sensitive to the form of the discharge pattern. This conclusion is further supported by the fact that taking Dykhne's model, which assumes quite a different discharge pattern (randomly distributed zones of high and low current densities) compared with the quasi-linear theory, and putting $\beta_{\text{eff}} \simeq \beta_{\text{crit}}$, which is a reasonable assumption (see Fig. 5), yields the result of the semiempirical expression Eq. (3d) for σ_{eff}, which is in good agreement with the theory. Furthermore, Eq. (3e) in its range of applicability $\beta_0 \gtrsim 7$ also coincides reasonably well with the experimental data, whereby the discharge pattern used (two orthogonal families of equidistant parallel striations oriented at $\pm\pi/4$ to the mean current direction) is different from the ones employed by Solbes or Dykhne. These considerations indicate that the initially mentioned inhomogeneities along the magnetic field lines should not have a serious influence on the plasma properties such as the effective electrical conductivity or electron temperature or electron number density.

b) Effective Hall Parameter

As already pointed out, the measurement of β_{eff} is not very precise mainly because of the difficulty in correctly determining the value of the angle γ. For comparison with the theory a case with a small value of γ is best suited because the influence of γ on β_{eff} is then less pronounced. This condition is met at high current densities. In Fig. 5 a value of 7 amp/cm² has been chosen for $\langle J \rangle$, which corresponds to a value of γ of $5° \pm 1°$. The error margins for β_{eff}, which are not given in Fig. 5, are $\pm 10\%$. In the stable region ($\langle \beta \rangle < \beta_{\text{crit}}$; $B = 1.1$ T) the agreement between theory and experiment is reasonably good, that is within the experimental accuracy. In the unstable region the qualitative behavior regarding the dependence of β_{eff} on the gas pressure and the magnetic induction is similar, but the absolute

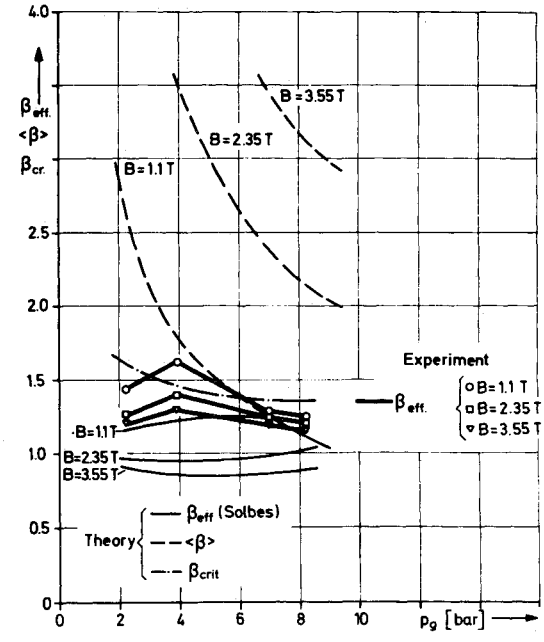

Fig. 5 Effective Hall parameters vs the gas pressure at constant current density $\langle J \rangle = 7$ amp/cm².

values for β_{eff} disagree to an extent which cannot be explained on the basis of the error margins. This disagreement is not in contradiction to the results of Ref. 4, where theory and experiment coincide surprisingly well. The reason for the good agreement in Ref. 4 is the fact that β_{crit}, which is an important parameter in calculating β_{eff}, was not taken from the theory, but was chosen such as to give the best fit to the experimental data considered using values for β_{crit} between 1.9 and 2.7, whereas β_{crit} according to the theory is lower, about 1.4. How the magnitude of β_{crit} affects the magnitude of β_{eff} can best be seen from the limiting case $\langle\beta\rangle \gg 1$, where β_{eff} according to Ref. 4 is given by

$$\beta_{eff} \simeq (\sigma_N^2 + \beta_{crit}^2)^{1/2} - 1$$

A possible explanation for the discrepancy between theory and experiment regarding the absolute value of β_{eff} could be the fact that the actual discharge pattern is more complicated than the one used in the theory, as already pointed out in the foregoing section. For an axial discharge it was shown in Ref. 19 that the striations, originally straight as assumed in the theory, become wavy owing to the influence of the boundary conditions when $\langle\beta\rangle$ exceeds β_{crit} by a factor of roughly 2. In a transverse discharge the presence of the streamers makes the discharge structure different from the one investigated in the theory. Considering our results, it looks as if the effective electrical conductivity is less sensitive to the form of the discharge pattern than the effective Hall parameter. In this context the inhomogeneities along the magnetic field lines could also play a role.

c) Electron Temperature and Electron Number Density

The electron temperature was measured as a function of the current density at a pressure of $p = 2.2$ bar and various magnetic inductions (Fig. 6). For $B = 3.25$ T the curves calculated with the relations Eqs. (3a, 3b, and 3d) are plotted, whereas for $B = 0$ and 1.6 T only those values obtained with Eq. (3b) are given. For the same reason as in the case of the effective electrical conductivity (Sec. Va) the curve representing Eq. (3e) has been omitted in Fig. 6 and also in Fig. 7. Within the given margins of error the experimental values agree with those calculated with all four relations [Eqs. (3a, 3b, 3d, and 3e)]. In keeping with the tendency observed in the conductivity values, however, the results obtained with Eq. (3a) deviate most from the experimental values. As expected, at constant current density the electron temperature is in the unstable plasma larger than in the stable plasma, the maximum difference being about 10% in the cases investigated here.

In the curves showing the relative electron density elevation due to ionization instabilities (Fig. 7) the values calculated with Eqs. (3b, 3d and, 3e) are again in good agreement with those

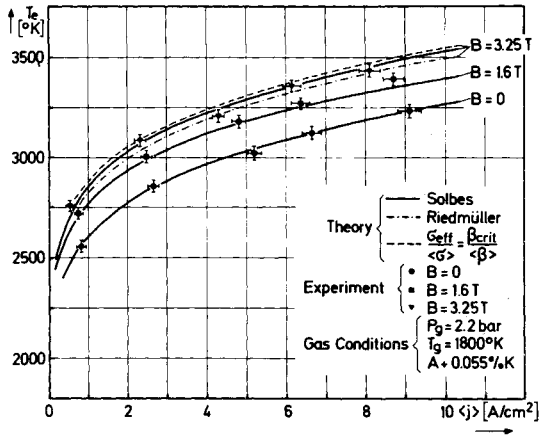

Fig. 6 Electron temperature as a function of the current density at various magnetic inductions ($p = 2.2$ bar).

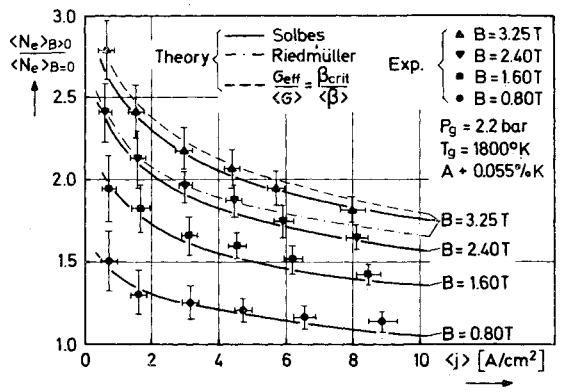

Fig. 7 Normalized electron density as a function of the current density at various magnetic inductions ($p = 2.2$ bar).

measured, as can be seen in the curves for $B = 3.25$ T, whereas the curves obtained with Eq. (3a) are outside the region defined by the margins of error. The curves derived from Eq. (3b) are plotted for $B = 0.8$, 1.6 and 2.4 T. These agree with the experimental values within the measuring accuracy. The electron temperature and density measurements thus also confirm that the relations Eqs. (3b, 3d, and 3e) describe the experimental conditions in good approximation, whereas the relation Eq. (3a) yields too high values of the effective conductivity at too low electron densities and temperatures. In the model on which Eq. (3a) is based the dissipation losses due to ionization instabilities are thus too low.

Summary

The question which of the available theories treating the influence of ionization instabilities on the various plasma properties describes the actual conditions in best approximation has been investigated.

It was found that Solbes' theory based on the quasi-linear analysis of plane ionization waves can reproduce the experimental data of the effective electrical conductivity, electron temperature, and electron number density within the measuring accuracy although the discharge pattern used in the theory is different from the one actually occurring because of the presence of the streamers. This seems to indicate that these plasma properties are not very sensitive to the form of the discharge pattern. The case is different, however, with the effective Hall parameter. Its measured value was about 30% larger than its theoretically calculated value.

Using the semiempirical expression $\sigma_{eff}/\langle\sigma\rangle = \beta_{crit}/\langle\beta\rangle$ or the formula $\sigma_{eff}/\sigma_0 = [\beta_{crit}/(2)^{1/2}\beta_0]^{1/2}$ as employed in Refs. 6 and 7 in its range of applicability $\beta_0 \gtrsim 5\beta_{crit} \simeq 7$ for the reduction of the effective electrical conductivity, it was also possible to achieve good agreement between theory and experiment regarding the effective electrical conductivity, the electron temperature and the electron number density. Moreover, by assuming a slightly ionized plasma in which the radiation losses can be neglected relative to the elastic losses the relation $\sigma_{eff}/\langle\sigma\rangle = \beta_{crit}/\langle\beta\rangle$ allows a reduced representation according to which all the different curves obtained for the effective electrical conductivity in the entire current density, pressure and magnetic field ranges investigated can be combined in one curve. The corresponding reduced experimental data lie on this curve.

The model suggested by Riedmüller slightly overestimates the actual effective electrical conductivity and consequently underestimates the rise of the electron temperature and electron number density caused by the ionization instability. This result comes from a different linearization process compared with Solbes' theory what finally results in an underestimation of the dissipation losses due to the ionization instabilities.

References

[1] Brederlow, G., Witte, K. J., and Zinko, H., "Investigation of the Discharge Structure in a Noble Gas Alkali MHD Generator Plasma," *AIAA Journal,* Vol. 11, No. 8, Aug. 1973, pp. 1065–1072.

[2] Brederlow, G., Witte, K. J., and Zinko, H., "Performance of a Faraday Rare Gas Alkali MHD Generator," *AIAA Journal,* to be published.

[3] Riedmüller, W., "The Effective Electrical Conductivity of a Non-equilibrium MHD Plasma," Rept. IPP IV/52, 1973, Max-Planck-Institut für Plasmaphysik, Garching, Germany.

[4] Solbes, A., "Quasilinear Plane Wave Study of Electrothermal Instabilities," *Proceedings of the International Symposium on MHD Electrical Power Generator,* Vol. I, Warsaw, 1968, p. 499.

[5] Dykhne, A. M., "Anomalous Plasma Resistance in a Strong Magnetic Field," *Soviet Physics JETP,* (English Translation), Vol. 32, No. 2, 1971, pp. 348–351.

[6] Velikhov, E. P., Degtyarev, L. M., and Favorskii, A. P., "Numerical Simulation of Ionization Instability," *Proceedings of the International Symposium on MHD Electrical Power Generator,* Vol. 2, Munich, 1971, pp. 307–322.

[7] Gay, P. and Zampaglione, V., "Investigation of the MHD Interaction in a Subsonic Generator with Turbulent Nonequilibrium Plasma," *13th Symposium on Engineering Aspects of MHD,* Stanford Univ., Stanford, Calif., 1973, pp. 121–125.

[8] Schwenn, R., Brederlow, G., and Salvat, M., "Electrical Conductivity of an Argon Potassium Plasma at Low Current Densities as a Function of the Gas Temperature," *Plasma Physics,* Vol. 10, 1968, pp. 1077–1099.

[9] Frost, L. S. and Phelps, A. V., "Momentum Transfer Cross Sections for Slow Electrons in He, Ar, Kr and Xe from Transport Coefficients," *Physics Review,* Vol. 136, No. 6A, 1964, pp. A1538–A1545.

[10] Sutton, G. W. and Sherman, A., *Engineering Magnetohydrodynamics,* McGraw-Hill, New York, 1965, p. 162.

[11] Raeder, J., private communication, 1973, Max-Planck-Institut für Plasmaphysik, Garching, Germany.

[12] Karule, E. and Peterkop, R., "Collisions of Slow Electrons with Alkali Atoms," *Proceedings of the 4th International Conference on the Physics of Electronic and Atomic Collisions,* Quebec, Canada, 1965, pp. 134–139.

[13] Karule, E., "Elastic Scattering of Low Energy Electrons by Alkali Atoms," *Proceedings of the 4th International Conference on the Physics of Electronic and Atomic Collisions,* Quebec, Canada, 1965, pp. 139–143.

[14] Visconti, P. J., Slevin, J. A. and Rubin, K., "Absolute Total Cross Section for the Scattering of Low Energy Electrons by Rubidium, Cesium and Potassium," *Physics Review,* Vol. A3, 1971, p. 1310.

[15] Collins, A. I., Bedexon, B., and Goldstein, M., "Differential Spin Exchange and the Elastic Scattering of Low Energy Electrons by Potassium," *Physics Review,* Vol. A3, 1971, p. 1976.

[16] Kruger, C. H., Mitchner, M., and Daybelge, U., "Transport Properties of MHD Generator Plasmas," *AIAA Journal,* Vol. 6, No. 9, June 1968, pp. 1712–1723.

[17] Riedmüller, W., Brederlow, G., and Salvat, M., "On the Applicability of the Line Reversal Method for Measuring the Electron Temperature in a Weakly Ionized Alkali Seeded Rare Gas Plasma," *Zeitschrift fuer Naturforsch,* Vol. 23a, 1968, p. 731.

[18] Agnew, L. and Summers, C., "Quantum Spectroscopy of Cesium Plasma," *Proceedings of the 7th International Conference on Phenomena in Ionized Gases,* Vol. II, Belgrade, 1966, pp. 574–580.

[19] Riedmüller, W., "Experimental and Theoretical Studies of the Influence of Boundary Conditions on the Development of Ionization Instability," *Proceedings of the 11th Symposium on Engineering Aspects of MHD,* California Inst. of Technology, Pasadena, Calif., 1970, pp. 199–204.